Published in final edited form as:
J Nucl Med. 2011 March ; 52(3): 470–477. doi:10.2967/jnumed.110.082826.

In Vitro and In Vivo Evaluation of ^{64}Cu-Labeled SarAr-Bombesin Analogs in Gastrin-Releasing Peptide Receptor–Expressing Prostate Cancer

Kimberly A. Lears[1], **Riccardo Ferdani**[2], **Kexian Liang**[2], **Alexander Zheleznyak**[2], **Rebecca Andrews**[1], **Christopher D. Sherman**[2], **Samuel Achilefu**[2], **Carolyn J. Anderson**[2], and **Buck E. Rogers**[1]

[1]Department of Radiation Oncology, Washington University School of Medicine, St. Louis, Missouri

[2]Mallinckrodt Institute of Radiology, Washington University School of Medicine, St. Louis, Missouri

Abstract

Bombesin is a 14–amino-acid amphibian peptide that binds with high affinity to the gastrin-releasing peptide receptor (GRPR), which is overexpressed on a variety of solid tumors. It has been demonstrated that bombesin analogs can be radiolabeled with a variety of radiometals for potential diagnosis and treatment of GRPR-positive tumors. In this regard, several studies have used different chelators conjugated to the 8 C-terminal amino acids of bombesin(7–14) for radiolabeling with ^{64}Cu. These analogs have demonstrated GRPR-specific small-animal PET of tumors but have various advantages and disadvantages. The objective of this study was to conjugate the previously described (1-*N*-(4-aminobenzyl)-3,6,10,13,16,19-hexaazabicyclo[6.6.6]-eicosane-1,8-diamine) (SarAr) chelator to bombesin (7–14), radiolabel the conjugate with ^{64}Cu, and evaluate in vitro and in vivo.

Methods—SarAr was synthesized as previously published and conjugated to bombesin(7–14) by solid-phase peptide synthesis using standard Fmoc chemistry. Succinic acid (SA), 8-aminooctanoic acid (Aoc), and Gly-Ser-Gly (GSG) were used as linkers between SarAr and bombesin(7–14) to yield the resulting SarAr-SA-Aoc-bombesin(7–14) and SarAr-SA-Aoc-GSG-bombesin(7–14) peptides. The unlabeled peptides were evaluated in a competitive binding assay using PC-3 prostate cancer cells and ^{125}I-Tyr^{4}-bombesin to determine the inhibitory concentration of 50%. The peptides were radiolabeled with ^{64}Cu and evaluated for internalization into PC-3 cells in vitro and for in vivo tumor uptake in mice bearing PC-3 xenografts using biodistribution and small-animal PET/CT studies.

Results—The competitive binding assay demonstrated that both SarAr-SA-Aoc-bombesin(7–14) and SarAr-SA-Aoc-GSG-bombesin(7–14) bound with high affinity to GRPR with an inhibitory concentration of 50% of 3.5 and 4.5 nM, respectively. Both peptides were radiolabeled with ^{64}Cu at room temperature without further purification and demonstrated similar internalization into PC-3 cells. In vivo, the radiolabeled peptides demonstrated tumor-specific uptake (13.0 and 8.5 percentage injected dose per gram for ^{64}Cu-SarAr-SA-Aoc-bombesin(7–14) and ^{64}Cu-SarAr-SA-Aoc-GSG-bombesin(7–14), respectively, at 1 h) and imaging that was comparable to, or better than, that of the previously reported ^{64}Cu-labeled bombesin analogs. The ^{64}Cu-SarAr-SA-Aoc-GSG-bombesin(7–14) had more rapid blood clearance and lower tumor and normal-tissue uptake

For correspondence or reprints contact: Buck E. Rogers, Department of Radiation Oncology, Washington University School of Medicine, 4511 Forest Park Blvd., Ste. 411, St. Louis, MO 63108. rogers@radonc.wustl.edu.

than ^{64}Cu-SarAr-SA-Aoc-bombesin(7–14), resulting in similar tumor-to-blood ratios for each analog (15.1 vs. 11.3 for ^{64}Cu-SarAr-SA-Aoc-bombesin(7–14) and ^{64}Cu-SarAr-SA-Aoc-GSG-bombesin(7–14), respectively, at 1 h).

Conclusion—These studies demonstrate that ^{64}Cu-SarAr-SA-Aoc-bombesin(7–14) and ^{64}Cu-SarAr-SA-Aoc-GSG-bombesin(7–14) bound with high affinity to GRPR-expressing cells and that these peptides can be used for PET of GRPR-expressing prostate cancer.

Keywords

oncology; peptides; PET/CT; radiopharmaceuticals; bombesin; ^{64}Cu; gastrin-releasing peptide receptor; small-animal PET/CT

The gastrin-releasing peptide receptor (GRPR) is a G-protein–coupled receptor that is overexpressed on a variety of tumors including prostate, breast, and small cell lung cancer (1,2). Bombesin is a 14–amino-acid amphibian homolog of the mammalian gastrin-releasing peptide and binds with high affinity to GRPR (3). Several bombesin analogs have been radiolabeled with various radionuclides for the development of diagnostic or therapeutic pharmaceuticals for targeting cancers that overexpress GRPR (4–11). In this regard, our laboratory has focused on the radiolabeling of bombesin analogs with the positron-emitting radionuclide ^{64}Cu (12–15). These studies have used the 8 C-terminal amino acids of bombesin(7–14) conjugated to the macrocyclic chelator DOTA, with numerous linkers between the peptide and DOTA. Although these studies have demonstrated GRPR-specific tumor uptake by biodistribution and small-animal PET, uptake in normal tissues such as the liver was high, resulting in low tumor–to– normal-tissue ratios.

The focus of this study was to determine whether these tumor–to–normal-tissue ratios could be improved by conjugating a chelator other than DOTA to bombesin(7–14) for complexing ^{64}Cu. Even though DOTA has been conjugated to many peptides and antibodies for radiolabeling with ^{64}Cu, it has been shown that ^{64}Cu can dissociate in vivo and transchelate to other proteins, leading to a high accumulation in nontarget tissues (16). Recently, 2 chelators, 1,4,8,11-tetraazabicyclo[6.6.2]hexadecane-4,11-diacetic acid (CB-TE2A) and 1,4,7-triazacyclononane-1,4,7-triacetic acid (NOTA), have been conjugated to bombesin(7–14) and compared directly with DOTA-conjugated bombesin(7–14) (17). The ^{64}Cu-labeled CB-TE2A conjugate demonstrated lower tumor uptake than the DOTA conjugate but also lower liver accumulation, leading to tumor-to-liver ratios approximately 6-fold better for the CB-TE2A conjugate at 4 h after injection (17). Similar results were obtained when comparing the ^{64}Cu-labeled NOTA conjugate to DOTA (18). In this study, we conjugated (1-*N*-(4-aminobenzyl)-3,6,10,13,16,19-hexaazabicyclo[6.6.6]-eicosane-1,8-diamine) (SarAr) to bombesin(7– 14) using 2 different linkers for radiolabeling with ^{64}Cu and determining the tumor uptake and normal-tissue clearance. SarAr has been shown to form rapid and stable complexes with ^{64}Cu and selective formation of Cu(II) complexes, compared with Co(II) and Ni(II) (19), and therefore was of interest to our group for radiolabeling of bombesin(7–14) analogs with ^{64}Cu.

The bombesin analogs, SarAr-succinic acid (SA)-8-aminooctanoic acid (Aoc)-bombesin(7–14) and SarAr-SA-Aoc-Gly-Ser-Gly (GSG)-bombesin(7–14), evaluated in this study are shown in Figure 1 and differ by an additional GSG spacer between Aoc and bombesin(7–14). These analogs were evaluated for binding to GRPR-positive PC-3 human prostate cancer cells and for internalization into these cells after radiolabeling with ^{64}Cu. The tumor localization and normal-tissue accumulation of the ^{64}Cu-labeled analogs were then determined using in vivo biodistribution and small-animal PET studies with mice bearing PC-3 xenografts.

MATERIALS AND METHODS

Synthesis of Bombesin Analogs

The chelator SarAr was synthesized as previously described (20) and stored as the nitro compound until it was ready for conjugation, at which point it was reduced to the aniline for conjugation to the bombesin peptides. Fmoc-Aoc was purchased from Advanced ChemTech. Amino acids and SA were purchased from Novabiochem. SA-Aoc-bombesin(7–14) and SA-Aoc-GSG-bombesin(7–14) were synthesized on solid support using automated standard Fmoc chemistry at room temperature. Starting with the methionine-loaded rink amide resin (30 μmol), subsequent amino acids were coupled to the resin using the appropriate Fmoc-protected amino acids (90 μmol) and coupling reagents 2-(1H–benzotriazole-1-yl)-1,1,3,3-tetramethyluronium hexafluorophosphate (90 μmol), 1-hydroxybenzotriazole (90 μmol), and *N*, *N*-diisopropylethylamine (180 μmol). Aoc was coupled by the same method, but conjugation of SA did not require the use of 2-(1H-benzotriazole-1-yl)-1,1,3,3-tetramethyluronium hexafluorophos-phate and 1-hydroxybenzotriazole activation reagents. The resin was thoroughly washed with *N*,*N*-dimethylformamide and dichloromethane and dried before activation of the free carboxylic acid of SA on the solid support with the coupling reagents. After 30 min, SarAr (180 μmol) in dry dimethyl sulfoxide (0.5 mL) and *N*,*N*-dimethylformamide (1.0 mL) under argon were added to the resin, and the mixture was stirred overnight. Cleavage of the peptide and concomitant removal of the side-chain protecting groups was obtained with 94% trifluoroacetic acid, 1% triisopropylsilane, 2.5% 1,2-ethanedithiol, and 2.5% water. The resulting product was purified by preparative high-performance liquid chromatography (HPLC) using a Grace Vydac C-18 column (250 × 21.2 mm). The desired compound was obtained by linear gradient elution consisting of solvents A (0.1% trifluoroacetic acid in water) and B (0.1% trifluoroacetic acid in acetonitrile) from 90% to 40% A for 18 min at 10 mL/min. The elution was monitored by ultraviolet absorbance at 214 and 254 nm. SarAr-SA-Aoc-GSG-bombesin(7–14) and SarAr-SA-Aoc-bombesin(7–14) were more than 95% pure by HPLC. Peptide identities were confirmed by electrospray mass spectrometry: SarAr-SA-Aoc-GSG-bombesin(7–14) ($C_{83}H_{134}N_{26}O_{16}S$), calculated (M+1) *m*/*z* 1,785.20; found 892.95 (M+2), 595.60 (M+3); SarAr-SA-Aoc-bombesin(7–14) ($C_{76}H_{123}N_{23}O_{12}S$), calculated (M+1) *m*/*z* 1,584.04; found 792.55 (M+2), 528.85 (M+3).

Competitive Binding Assay

The inhibitory concentrations of 50% (IC_{50}) of SarAr-SA-Aoc-bombesin(7–14) and SarAr-SA-Aoc-GSG-bombesin(7–14) were determined using a competitive binding assay with ^{125}I-Tyr^4-bombesin (PerkinElmer). PC-3 human prostate adenocarcinoma cells were obtained from the American Type Tissue Culture Center and maintained in 45% RPMI 1640, 45% Ham's F-12, and 10% heat-inactivated fetal bovine serum. The medium components were obtained from Invitrogen, and the fetal bovine serum was obtained from Sigma Chemical Co. The cells were seeded in 6-well plates (5×10^5 cells per well) and incubated at 37°C overnight. The medium was then replaced with 1 mL of Dulbecco's modified Eagle's medium and 1% fetal bovine serum containing various amounts of SarAr-SA-Aoc-bombesin(7–14) and SarAr-SA-Aoc-GSG-bombesin(7–14) in triplicate such that the final concentration ranged from 5 pM to 0.5 μM. ^{125}I-Tyr^4-bombesin (final concentration, 0.05 nM) was then added to each well, and the plates were incubated at 4°C for 2 h. The cells were then rinsed twice with ice-cold phosphate-buffered saline and harvested. The cells were placed on a γ-counter (Packard II; PerkinElmer) to determine the cell-associated radioactivity. The data were plotted with Prism software (version 4; GraphPad Software) using the sigmoidal dose–response equation, with counts per minute of radioactivity bound versus log of the concentration of SarAr-SA-Aoc-bombesin(7–14) and SarAr-SA-Aoc-GSG-bombesin(7– 14) for the determination of the IC_{50}.

Radiolabeling of Bombesin Analogs

^{64}Cu (half-life, 12.7 h; positron energy, 0.656 MeV, 17.8%) was produced on a biomedical cyclotron at Washington University in St. Louis, as previously described (21). The bombesin analogs were radiolabeled with ^{64}Cu by diluting $^{64}CuCl_2$ with at least a 10-fold excess of 0.1 M NH_4OAc (pH 5.5), and then 37–74 MBq were added to 5–10 μg of SarAr-SA-Aoc-bombesin(7–14) and SarAr-SA-Aoc-GSG-bombesin(7–14) in a total volume of approximately 100 μL. The reaction mixtures were then incubated at room temperature for 30 min, and the radiochemical purity was determined by radio–thin-layer chromatography. One microliter of the reaction mixtures was applied to MKC18F reversed-phase thin-layer chromatography plates (Whatman Inc.) and developed with 10% ammonium acetate:methanol (30:70) as the mobile phase. The thin-layer chromatography plates were scanned on a BioScan Imaging Scanner, and the radiolabeled peptides were used immediately without purification for in vitro and in vivo assays.

Internalization of Bombesin Analogs

PC-3 cells (5×10^5) were plated in 6-well plates and incubated overnight at 37°C. The cells were then washed twice with Hanks balanced salt solution, followed by the addition of 1 mL of Dulbecco's modified Eagle's medium containing 30 mM *N*-(2-hydrox-yethyl)piperazine-*N*′-(2-ethanesulfonic acid), 2 mM L-glutamine, 1 mM sodium pyruvate, and 1% bovine serum albumin. Tyr^4-bombesin (10 μg; Sigma Chemical Co.) was added to 3 of the 6 wells per plate to act as a blocking agent, followed immediately by the addition of ^{64}Cu-SarAr-SA-Aoc-bombesin(7–14) or ^{64}Cu-SarAr-SA-Aoc-GSG-bombesin(7–14) (18.5 kBq) such that the final concentration of radiolabeled peptide was 1 nM. The plates were then incubated at 37°C for various times (15, 30 60, 120, 240, and 1,200 min), at which point they were removed from the incubator and washed twice with Hanks balanced salt solution. The cells were then washed twice with 500 μL of 20 mM sodium acetate in Hanks balanced salt solution, pH 4.0, to remove surface-bound radioactivity, and these washes were discarded. The cells were then harvested using 1% sodium dodecyl sulfate in 10 mM sodium borate and placed on the γ-counter to determine the amount of internalized radioactivity. The counts per minute internalized were converted to femtomoles on the basis of the specific activity of the peptides and normalized to the protein in each well as determined using a BCA Protein Kit (Pierce). The data are presented as the specific amount (femtomoles in nonblocked wells minus femtomoles in blocked wells) of radiolabeled peptide internalized per milligram of protein versus time.

Biodistribution Studies

All animal studies were performed under the *Guide for the Care and Use of Laboratory Animals* (22) through the Washington University Animal Studies Committee. PC-3 cells in phosphate-buffered saline were mixed 1:1 (v:v) with Matrigel Basement Membrane Matrix (Becton Dickinson), and 200 μL (1×10^7 cells) were injected subcutaneously into 3- to 4-wk-old female CB.17 severe combined immune-deficient mice (Charles River Laboratories). The tumors were allowed to grow for 27 d (tumor weight, ~250 mg), and the mice ($n = 5$ per group) were injected intravenously with 0.6 MBq (70 ng) of either ^{64}Cu-SarAr-SA-Aoc-bombesin(7–14) or ^{64}Cu-SarAr-SA-Aoc-GSG-bombesin(7– 14). The mice were sacrificed at 1, 4, or 24 h later, and the blood, lungs, liver, spleen, kidneys, muscle, bone, pancreas, and tumor were harvested, weighed, and counted in the γ-counter. An additional group of mice was injected with the radiolabeled bombesin analogs premixed with 100 μg of Tyr^4-bombesin to serve as a blocking agent and sacrificed at 1 h. The percentage injected dose per gram of tissue (%ID/g) was determined by decay correction of the ^{64}Cu-labeled bombesin analogs for each sample normalized to a standard of known weight, which was representative of the injected dose.

Small-Animal PET/CT Studies

PC-3 cells were implanted in severe combined immune-deficient mice. The mice (n = 3) were injected intravenously with 5.6 MBq (675 ng) of ^{64}Cu-SarAr-SA-Aoc-bombesin(7–14) or ^{64}Cu-SarAr-SA-Aoc-GSG-bombesin(7–14) with or without 100 μg of Tyr^4-bombesin. At 1, 4, and 24 h after injection, the mice were anesthetized with 1%–2% isoflurane, positioned supine, and imaged on microPET Focus 120/220 or Inveon PET small-animal scanners (Siemens Medical Solutions). The PET acquisition times were 10 min for the 1- and 4-h times and 20 min for the 24-h time. CT images were obtained using a MicroCAT II System (ImTek, Inc.). The images were reconstructed with an ordered-subset estimation maximization algorithm, which included corrections for scatter and attenuation. Regions of interest were drawn to encompass the entire tumor to determine the maximum activity concentration (Bq/cm^3) in the tumor. To calculate the standardized uptake values, the Becquerels per cubic centimeter were divided by the Becquerels injected (decay corrected to the scan start time) and multiplied by the mouse weight.

Statistical Analysis

All data are presented as the mean ± SEM. The Student 2-tailed t test was used to determine statistical significance at the 95% confidence level, with a P value of 0.05 or less being considered significantly different.

RESULTS

Competitive Binding Assay

Representative competitive binding curves of SarAr-SA-Aoc-bombesin(7–14) and SarAr-SA-Aoc-GSG-bombesin (7–14) are shown in Figure 2. The binding of ^{125}I-Tyr^4-bombesin to PC-3 cells was inhibited by various concentrations of SarAr-SA-Aoc-bombesin(7–14) and SarAr-SA-Aoc-GSG-bombesin(7–14). The IC_{50} values for SarAr-SA-Aoc-bombesin(7–14) and SarAr-SA-Aoc-GSG-bombesin(7–14) were 3.5 ± 0.5 and 4.5 ± 0.8 nM, respectively, and are not significantly different.

Radiolabeling and Internalization

Both bombesin analogs were radiolabeled with ^{64}Cu at room temperature in more than 95% radiochemical purity and at a specific activity of 12.4 GBq/μmol for internalization, biodistribution, and imaging studies. Figure 3 shows that the internalization of ^{64}Cu-SarAr-SA-Aoc-bombesin(7–14) was similar to the internalization of ^{64}Cu-SarAr-SA-Aoc-GSG-bombesin(7–14), with no significant differences in the amount internalized at any of the time points. Curve fitting showed that the maximum internalizations were 686 and 771 fmol/mg for ^{64}Cu-SarAr-SA-Aoc-bombesin(7–14) and ^{64}Cu-SarAr-SA-Aoc-GSG-bombesin (7–14), respectively. The initial velocities of internalization were 2.6 and 3.2 fmol/mg/min for ^{64}Cu-SarAr-SA-Aoc-bombesin(7–14) and ^{64}Cu-SarAr-SA-Aoc-GSG-bombesin (7–14), respectively, as determined by linear regression of the data from 0 to 60 min.

Biodistribution Studies

Table 1 shows the %ID/g values for ^{64}Cu-SarAr-SA-Aoc-bombesin(7–14) and ^{64}Cu-SarAr-SA-Aoc-GSG-bombesin(7–14) in various tissues at 1, 4, and 24 h. The blood concentrations of ^{64}Cu-SarAr-SA-Aoc-bombesin(7–14) and ^{64}Cu-SarAr-SA-Aoc-GSG-bombesin(7–14) were not significantly different at 1 h but were significantly different (P < 0.005) at 4 and 24 h, with ^{64}Cu-SarAr-SA-Aoc-GSG-bombesin(7–14) having less than half the blood activity of ^{64}Cu-SarAr-SA-Aoc-bombesin(7–14) at the later times. Compared with ^{64}Cu-SarAr-SA-Aoc-bombesin(7–14), ^{64}Cu-SarAr-SA-Aoc-GSG-bombesin(7–14) had significantly lower liver (P < 0.004), pancreas (P < 0.05), and tumor (P < 0.03) uptake at all times except for

the pancreas at 24 h. For lungs, spleen, kidneys, and muscle, the only significant differences between ^{64}Cu-SarAr-SA-Aoc-bombesin(7–14) and ^{64}Cu-SarAr-SA-Aoc-GSG-bombesin(7–14) were in the lungs at 4 and 24 h ($P < 0.003$) and the kidneys at 4 h ($P < 0.006$).

The tumor-to-blood, tumor-to-liver, tumor-to-kidney, and tumor-to-muscle ratios are shown in Figure 4. Although the tumor uptake was greater for ^{64}Cu-SarAr-SA-Aoc-bombesin(7–14) than for ^{64}Cu-SarAr-SA-Aoc-GSG-bombesin (7–14), the tumor–to–normal-tissue ratios were not significantly different between the 2 compounds at any time. The tumor uptake for ^{64}Cu-SarAr-SA-Aoc-bombesin(7–14) and ^{64}Cu-SarAr-SA-Aoc-GSG-bombesin(7–14) at 1 h was GRPR-mediated, as the inhibitor significantly reduced ($P < 0.002$) the tumor uptake for both (3.0 ± 0.4 %ID/g for ^{64}Cu-SarAr-SA-Aoc-bombesin(7–14) and 2.7 ± 0.2 %ID/g for ^{64}Cu-SarAr-SA-Aoc-GSG-bombesin(7–14)). Similarly, the pancreas uptake was significantly reduced ($P < 0.0004$) to 3.2 ± 0.2 %ID/g for ^{64}Cu-SarAr-SA-Aoc-bombesin (7–14) and 1.9 ± 0.1 %ID/g for ^{64}Cu-SarAr-SA-Aoc-GSG-bombesin(7–14).

Small-Animal PET/CT Studies

Small-animal PET/CT images of ^{64}Cu-SarAr-SA-Aoc-bombesin(7–14) and ^{64}Cu-SarAr-SA-Aoc-GSG-bombesin (7–14) at 1, 4, and 24 h are shown in Figure 5. Coronal views of maximum-intensity projections of 2 mice (one receiving blocking agent and the other not receiving blocking agent) from the fused PET/CT images for mice bearing PC-3 xenografts are shown in this figure. The mice on the right in each panel received 100 μg of Tyr^4-bombesin as a blocking agent, and the mice on the left did not. Tumor uptake is observed at all times in the mice that did not receive the blocking agent, whereas mice that received the blocking agent show less uptake in tumors. Clearance of both bombesin analogs through the kidneys and bladder is shown at 1 h, whereas at 4 h less activity is observed for ^{64}Cu-SarAr-SA-Aoc-GSG-bombesin(7–14) than for ^{64}Cu-SarAr-SA-Aoc-bombesin(7–14). Figure 6 shows the standardized uptake value analysis from the PET/CT studies, demonstrating that the tumor uptake was not significantly different between ^{64}Cu-SarAr-SA-Aoc-bombesin(7–14) and ^{64}Cu-SarAr-SA-Aoc-GSG-bombesin(7–14) at 1 and 4 h but that ^{64}Cu-SarAr-SA-Aoc-GSG-bombesin(7–14) was significantly less ($P < 0.04$) than ^{64}Cu-SarAr-SA-Aoc-bombesin (7–14) at 24 h. The tumor uptake of ^{64}Cu-SarAr-SA-Aoc-bombesin(7–14) was significantly reduced ($P < 0.04$) at all times in the presence of the blocking agent, whereas for ^{64}Cu-SarAr-SA-Aoc-GSG-bombesin(7–14) it was only significantly reduced at 24 h ($P < 0.02$).

DISCUSSION

The purpose of this study was to evaluate bombesin(7–14) radiolabeled with ^{64}Cu using SarAr as a chelator for targeting GRPR expressed on PC-3 cells. Our previous studies used DOTA conjugated to bombesin(7–14) via the Aoc linker. For this study, because the aniline on SarAr could not be coupled directly to the N-terminal amine of Aoc-bombesin(7–14) by solid-phase synthesis, we used SA as a bifunctional linker to conjugate SarAr to Aoc-bombesin (7–14). For comparison, we also synthesized an analog containing a GSG spacer to determine the effect of the hydrophilic serine on tumor uptake and normal-tissue clearance. Both of these analogs were synthesized on solid support and purified by HPLC after cleavage. Recently, Cai et al. described the synthesis of a new chelator, AmBaSar, that is similar to SarAr except that the aniline was replaced with benzoic acid for direct coupling to N-terminal amines or lysines (23,24). They demonstrated that AmBaSar could be easily coupled to the lysine of a cyclic arginine-glycine-aspartic acid (RGD) analog (c(RGDyk)) and radiolabeled with ^{64}Cu at room temperature (23). Ma et al. have also constructed a derivative of Sar by reacting copper-Sar with glutaric anhydride to obtain a carboxylic acid functionality that was conjugated to the lysine on Lys^3-bombesin (25).

When screened against the GRPR-expressing PC-3 cells, the analogs had IC_{50} values that were not significantly different ($P = 0.34$) and were better than other DOTA-con-jugated bombesin analogs evaluated in our laboratory (IC_{50} range, ~20–80 nM) (13,15). Efficient radiolabeling of the analogs with ^{64}Cu was achieved at room temperature, similar to when the NOTA chelator was conjugated to bombesin(7–14) (26), but differing from the heating at 70°C when using the CB-TE2A chelator (17). The internalization of ^{64}Cu-SarAr-SA-Aoc-bombesin(7–14) at 15 min was 54% of the value at 2 h, whereas the internalization of ^{64}Cu-SarAr-SA-Aoc-GSG-bombesin(7–14) at 15 min was 43%. These values are similar to the approximately 60% that Garrison et al. have shown for ^{64}Cu-CB-TE2A–Aoc-bombesin(7–14) in PC-3 cells (17). Although it has not been explicitly demonstrated in this study, it is assumed that the analogs evaluated here are agonists based on their structure and ability to internalize. Although traditional thinking has assumed that internalizing radiolabeled bombesin agonists are preferred to noninternalizing antagonists because of residualization of the radioactivity in tumor cells, recent publications using bombesin antagonists and other radiolabeled peptide antagonists have suggested otherwise (9,27,28). Therefore, it will be interesting to evaluate SarAr-conjugated bombesin antagonists for PET with ^{64}Cu in future studies.

The PC-3 tumor uptake (Table 1) of 8.5 %ID/g for ^{64}Cu-SarAr-SA-Aoc-GSG-bombesin(7–14) and 13.0 %ID/g for ^{64}Cu-SarAr-SA-Aoc-bombesin(7–14) at 1 h is higher than the approximate 2.8%–5.5 %ID/g that we and others have previously reported in this tumor model using DOTA as a chelator and various linkers (13,14,17,29). The ^{64}Cu-labeled analogs using the CB-TE2A and NOTA chelators had 2.7%–3.6 %ID/g in PC-3 tumors at 1 h after injection (17,18). Only bombesin antagonists radiolabeled with ^{99m}Tc or ^{111}In have had higher tumor uptakes in this model at 1 h, with a range of approximately 14–25 %ID/g (9,27,30). However, the liver uptakes of 5.1 %ID/g for ^{64}Cu-SarAr-SA-Aoc-GSG-bombesin(7–14) and 9.5 %ID/g for ^{64}Cu-SarAr-SA-Aoc-bombesin(7–14) at 1 h in this study were similar to what we have found with other analogs using the DOTA chelator and greater than the approximately 1.5–2 %ID/g that has been reported for CB-TE2A and NOTA chelators (17,18). Only 3% and 8% of the radioactivity remained in the blood at 24 h, compared with at 1 h for ^{64}Cu-SarAr-SA-Aoc-GSG-bombesin(7–14) and ^{64}Cu-SarAr-SA-Aoc-bombesin(7–14), respectively. This is much better than the 35%-98% retention in the blood for other analogs using the DOTA chelator (13,17) and comparable to the 10% retention when using the CB-TE2A chelator (17). The blood, liver, tumor, and pancreas clearance was more rapid for ^{64}Cu-SarAr-SA-Aoc-GSG-bombesin(7–14) than for ^{64}Cu-SarAr-SA-Aoc-bombesin(7–14). This finding was likely due to the increased hydrophilicity from the GSG linker, indicating that further modifications could be made to alter the pharmacokinetics of the SarAr-bombesin analogs.

The tumor-to-liver and tumor-to-kidney ratios ranged from 1.3 to 1.7 at all times for both ^{64}Cu-labeled SarAr analogs in this study (Fig. 4), which is better than the 0.6–1.2 that we previously reported for other ^{64}Cu-labeled analogs (13,14). The ^{64}Cu-CB-TE2A-Aoc-bombesin(7–14) had tumor-to-liver ratios (1.2–2.0 for 1–24 h) similar to those reported here but lower tumor-to-kidney ratios (0.5– 1.0) (17). The ^{64}Cu-NOTA-Aoc-bombesin(7–14) appears to have tumor-to-liver and tumor-to-kidney ratios similar to those that we have reported here (18). The tumor-to-blood and tumor-to-muscle ratios of approximately 11–182 and approximately 20–96, respectively, for the analogs reported here are much better than ^{64}Cu-CB-TE2A–Aoc-bombesin (7–14), which were approximately 5–20 for blood and approximately 2–14 for muscle; these ratios were not reported for ^{64}Cu-NOTA-Aoc-bombesin(7–14) (17,18).

Although the tumor-to-liver and tumor-to-kidney ratios reported in this study are improved relative to our previous publications and comparable to other ^{64}Cu-labeled BN analogs, this

improvement is mainly due to increased tumor uptake of ^{64}Cu-SarAr-SA-Aoc-bombesin(7–14) and ^{64}Cu-SarAr-SA-Aoc-GSG-bombesin(7–14). In general, blood and muscle clearance are more rapid for ^{64}Cu-SarAr-SA-Aoc-bombesin(7–14) and ^{64}Cu-SarAr-SA-Aoc-GSG-bombesin (7–14) than for our previously studied DOTA analogs, yet clearance from the other normal tissues is similar. It is not expected that the slow clearance from normal tissues is due to demetallation of ^{64}Cu from the SarAr chelator, because it has been previously shown that SarAr and similar chelators form complexes with ^{64}Cu that are stable in vivo (19,24,31). Cai et al. showed significantly less liver, stomach, and intestine uptake for ^{64}Cu-AmBaSar than for ^{64}Cu-DOTA at 2 h after injection in mice (24), whereas Smith showed significantly less liver uptake of ^{64}Cu-labeled Sar, 1,8-diamine-3,6,10,13,16,19-hexaazabicyclo[6.6.6]icosane, and SarAr than for free ^{64}Cu at 30 min (19). Cai et al. also showed that there was significantly less liver uptake of ^{64}Cu-AmBaSar-RGD than of ^{64}Cu-DOTA-RGD and that ^{64}Cu-AmBaSar-RGD remained intact in the blood, tumor, liver, and kidneys at 1 h by HPLC whereas intact ^{64}Cu-DOTA-RGD showed a significant loss (31). Conversely, Wei et al. showed that 96% of the radioactivity remained in the liver at 24 h, compared with 1 h, using 1,8-diamine-3,6,10,13,16,19-hexaazabicyclo [6.6.6]icosane conjugated to a cyclic RGD peptide, whereas only 22% remained when a similar peptide and the CB-TE2A chelator were used (32). The ^{64}Cu-NOTA-Aoc-bombesin(7–14) and ^{64}Cu-CB-TE2A–Aoc-bombesin(7–14) both exhibited rapid tumor and normal-tissue clearance (17,18). The aggregate of these findings suggests that metabolism studies should be performed in the future to confirm that ^{64}Cu is not being released from the SarAr-conjugated bombesin analogs and to elucidate a possible mechanism for the retention of radioactivity in normal tissues.

The PET/CT images (Fig. 5) show distinct GRPR-mediated uptake of ^{64}Cu-SarAr-SA-Aoc-bombesin(7–14) and ^{64}Cu-SarAr-SA-Aoc-GSG-bombesin(7–14) in the PC-3 flank tumors (mice on the left), as evidenced by the lack of tumor uptake in the mice that received the radiopharma-ceuticals with a coinjection of blocking agent (mice on the right). These images show clearance of the radioactivity through the kidneys and bladder for both analogs, with ^{64}Cu-SarAr-SA-Aoc-GSG-bombesin(7–14) clearing more rapidly than ^{64}Cu-SarAr-SA-Aoc-bombesin(7–14) and ^{64}Cu-SarAr-SA-Aoc-GSG-bombesin(7–14), as observed in the biodistribution studies. Figure 6 shows that the tumor uptake of ^{64}Cu-SarAr-SA-Aoc-bombesin(7–14) was significantly decreased at all times when coinjected with the blocking agent ($P < 0.04$), whereas the decrease for ^{64}Cu-SarAr-SA-Aoc-GSG-bombesin(7–14) was significant only at 24 h ($P < 0.02$). Heterogeneity of uptake within the tumor can be observed and was correlated with anatomic information from MRI in a multimodality imaging study recently reported by Prasanphanich et al. (26). This multimodality imaging would allow the identification of low-receptor-density areas that could aid the design and evaluation of targeted therapeutics.

CONCLUSION

We have shown that the copper chelator SarAr can be coupled to bombesin(7–14) with retention of affinity to GRPR on PC-3 prostate cancer cells. The resulting conjugates were readily labeled with ^{64}Cu and demonstrated rapid internalization into PC-3 cells. The tumor uptake is among the highest reported for radiolabeled BN agonists; however, there is still considerable retention of radioactivity in normal tissues. The tumor–to–normal-tissue ratios are comparable to the best ^{64}Cu-labeled bombesin agonist analogs reported in the literature. These analogs should be useful for the detection or treatment of GRPR-expressing prostate cancers but could be optimized further to increase their normal-tissue clearance.

Acknowledgments

We gratefully acknowledge Margaret Morris, Nicole Fettig, Lori Strong, and Amanda Roth for performing the small-animal imaging studies. In addition, we thank Dr. Richard LaForest for his assistance in analyzing the imaging data and Jesse Parry and Dr. Jeffrey Craft for their critical reading of the manuscript. This work was supported by the Department of Radiation Oncology, Washington University School of Medicine, and NIH grants R01 CA136695 and 5R01 CA093375.

REFERENCES

1. Markwalder R, Reubi JC. Gastrin-releasing peptide receptors in the human prostate: relation to neoplastic transformation. Cancer Res. 1999; 59:1152–1159. [PubMed: 10070977]
2. Reubi JC, Wenger S, Schmuckli-Maurer J, Schaer JC, Gugger M. Bombesin receptor subtypes in human cancers: detection with the universal radioligand ^{125}I-[d-TYR^{6}, β-ALA^{11}, PHE^{13}, NLE^{14}] bombesin(6–14). Clin Cancer Res. 2002; 8:1139–1146. [PubMed: 11948125]
3. Anastasi A, Erspamer V, Bucci M. Isolation and structure of bombesin and alytesin, 2 analogous active peptides from the skin of the European amphibians Bombina and Alytes. Experientia. 1971; 27:166–167. [PubMed: 5544731]
4. Breeman WAP, de Jong M, Erion JL, et al. Preclinical comparison of ^{111}In-labeled DTPA- or DOTA-bombesin analogs for receptor-targeted scintigraphy and radionuclide therapy. J Nucl Med. 2002; 43:1650–1656. [PubMed: 12468515]
5. Hoffman TJ, Smith CJ. True radiotracers: Cu-64 targeting vectors based upon bombesin peptide. Nucl Med Biol. 2009; 36:579–585. [PubMed: 19647163]
6. Johnson CV, Shelton T, Smith CJ, et al. Evaluation of combined ^{177}Lu-DOTA-8-AOC-BBN(7–14)NH_2 GRP receptor-targeted radiotherapy and chemotherapy in PC-3 human prostate tumor cell xenografted SCID mice. Cancer Biother Radio-pharm. 2006; 21:155–166.
7. Lin KS, Luu A, Baidoo KE, et al. A new high affinity technetium-99m–bombesin analogue with low abdominal accumulation. Bioconjug Chem. 2005; 16:43–50. [PubMed: 15656574]
8. Maddalena ME, Fox J, Chen J, et al. ^{177}Lu-AMBA biodistribution, radiotherapeutic efficacy, imaging, and autoradiography in prostate cancer models with low GRP-R expression. J Nucl Med. 2009; 50:2017–2024. [PubMed: 19910427]
9. Mansi R, Wang X, Forrer F, et al. Evaluation of a 1,4,7,10-tetraazacyclododecane-1,4,7,10-tetraacetic acid-conjugated bombesin-based radioantagonist for the labeling with single-photon emission computed tomography, positron emission tomography, and therapeutic radionuclides. Clin Cancer Res. 2009; 15:5240–5249. [PubMed: 19671861]
10. Smith CJ, Volkert WA, Hoffman TJ. Radiolabeled peptide conjugates for targeting of the bombesin receptor superfamily subtypes. Nucl Med Biol. 2005; 32:733–740. [PubMed: 16243649]
11. Zhang H, Chen J, Waldherr C, et al. Synthesis and evaluation of bombesin derivatives on the basis of pan-bombesin peptides labeled with indium-111, lutetium-177, and yttrium-90 for targeting bombesin receptor-expressing tumors. Cancer Res. 2004; 64:6707–6715. [PubMed: 15374988]
12. Parry JJ, Andrews R, Rogers BE. MicroPET imaging of breast cancer using radiolabeled bombesin analogs targeting the gastrin-releasing peptide receptor. Breast Cancer Res Treat. 2007; 101:175–183. [PubMed: 16838112]
13. Parry JJ, Kelly TS, Andrews R, Rogers BE. In vitro and in vivo evaluation of ^{64}Cu-labeled DOTA-linker-bombesin(7–14) analogues containing different amino acid linker moieties. Bioconjug Chem. 2007; 18:1110–1117. [PubMed: 17503761]
14. Rogers BE, Bigott HM, McCarthy DW, et al. MicroPET imaging of a gastrinreleasing peptide receptor-positive tumor in a mouse model of human prostate cancer using a ^{64}Cu-labeled bombesin analog. Bioconjug Chem. 2003; 14:756–763. [PubMed: 12862428]
15. Rogers BE, Della Manna D, Safavy A. In vitro and in vivo evaluation of a ^{64}Cu-labeled polyethylene glycol bombesin conjugate. Cancer Biother Radiopharm. 2004; 19:25–34. [PubMed: 15068608]
16. Boswell CA, Sun X, Niu W, et al. Comparative in vivo stability of copper-64-labeled cross-bridged and conventional tetraazamacrocyclic complexes. J Med Chem. 2004; 47:1465–1474. [PubMed: 14998334]

17. Garrison JC, Rold TL, Sieckman GL, et al. In vivo evaluation and small-animal PET/CT of a prostate cancer mouse model using ^{64}Cu bombesin analogs: side-by-side comparison of the CB-TE2A and DOTA chelation systems. J Nucl Med. 2007; 48:1327–1337. [PubMed: 17631556]
18. Prasanphanich AF, Nanda PK, Rold TL, et al. [^{64}Cu-NOTA-8-Aoc-BBN(7–14) NH_2] targeting vector for positron-emission tomography imaging of gastrin-releasing peptide receptor-expressing tissues. Proc Natl Acad Sci USA. 2007; 104:12462–12467. [PubMed: 17626788]
19. Smith SV. Sarar technology for the application of copper-64 in biology and materials science. Q J Nucl Med Mol Imaging. 2008; 52:193–202. [PubMed: 18174877]
20. Di Bartolo NM, Sargeson AM, Donlevy TM, Smith SV. Synthesis of a new cage ligand, SarAr, and its complexation with selected transition metal ions for potential use in radioimaging. J Chem Soc, Dalton Trans. 2001:2303–2309.
21. McCarthy DW, Shefer RE, Klinkowstein RE, et al. Efficient production of high specific activity ^{64}Cu using a biomedical cyclotron. Nucl Med Biol. 1997; 24:35–43. [PubMed: 9080473]
22. Guide for the Care and Use of Laboratory Animals. Washington, DC: National Academy Press; 1996.
23. Cai H, Fissekis J, Conti PS. Synthesis of a novel bifunctional chelator AmBaSar based sarcophagine for peptide conjugation and ^{64}Cu radiolabelling. J Chem Soc, Dalton Trans. 2009:5395–5400.
24. Cai H, Li Z, Huang CW, Park R, Shahinian AH, Conti PS. An improved synthesis and biological evaluation of a new cage-like bifunctional chelator, 4-((8-amino-3,6,10,13,16,19-hexaazabicyclo[6.6.6]icosane-1-ylamino)methyl)benzoic acid, for ^{64}Cu radiopharmaceuticals. Nucl Med Biol. 2010; 37:57–65. [PubMed: 20122669]
25. Ma MT, Karas JA, White JM, Scanlon D, Donnelly PS. A new bifunctional chelator for copper radiopharmaceuticals: a cage amine ligand with a carboxy-late functional group for conjugation to peptides. Chem Commun. 2009:3237–3239.
26. Prasanphanich AF, Retzloff L, Lane SR, et al. In vitro and in vivo analysis of [^{64}Cu-NO2A-8-Aoc-BBN(7–14)NH_2]: a site-directed radiopharmaceutical for positron-emission tomography imaging of T-47D human breast cancer tumors. Nucl Med Biol. 2009; 36:171–181. [PubMed: 19217529]
27. Cescato R, Maina T, Nock B, et al. Bombesin receptor antagonists may be preferable to agonists for tumor targeting. J Nucl Med. 2008; 49:318–326. [PubMed: 18199616]
28. Ginj M, Zhang H, Waser B, et al. Radiolabeled somatostatin receptor antagonists are preferable to agonists for in vivo peptide receptor targeting of tumors. Proc Natl Acad Sci USA. 2006; 103:16436–16441. [PubMed: 17056720]
29. Yang YS, Zhang X, Xiong Z, Chen X. Comparative in vitro and in vivo evaluation of two ^{64}Cu-labeled bombesin analogs in a mouse model of human prostate adenocarcinoma. Nucl Med Biol. 2006; 33:371–380. [PubMed: 16631086]
30. Nock B, Nikolopoulou A, Chiotellis E, et al. [^{99m}Tc]Demobesin 1, a novel potent bombesin analogue for GRP receptor-targeted tumour imaging. Eur J Nucl Med Mol Imaging. 2003; 30:247–258. [PubMed: 12552343]
31. Cai H, Li Z, Huang CW, et al. Evaluation of copper-64 labeled AmBaSar conjugated cyclic RGD peptide for improved microPET imaging of integrin $\alpha_v\beta_3$ expression. Bioconjug Chem. 2010; 21:1417–1424. [PubMed: 20666401]
32. Wei L, Ye Y, Wadas TJ, et al. ^{64}Cu-labeled CB-TE2A and diamsar-conjugated RGD peptide analogs for targeting angiogenesis: comparison of their biological activity. Nucl Med Biol. 2009; 36:277–285. [PubMed: 19324273]

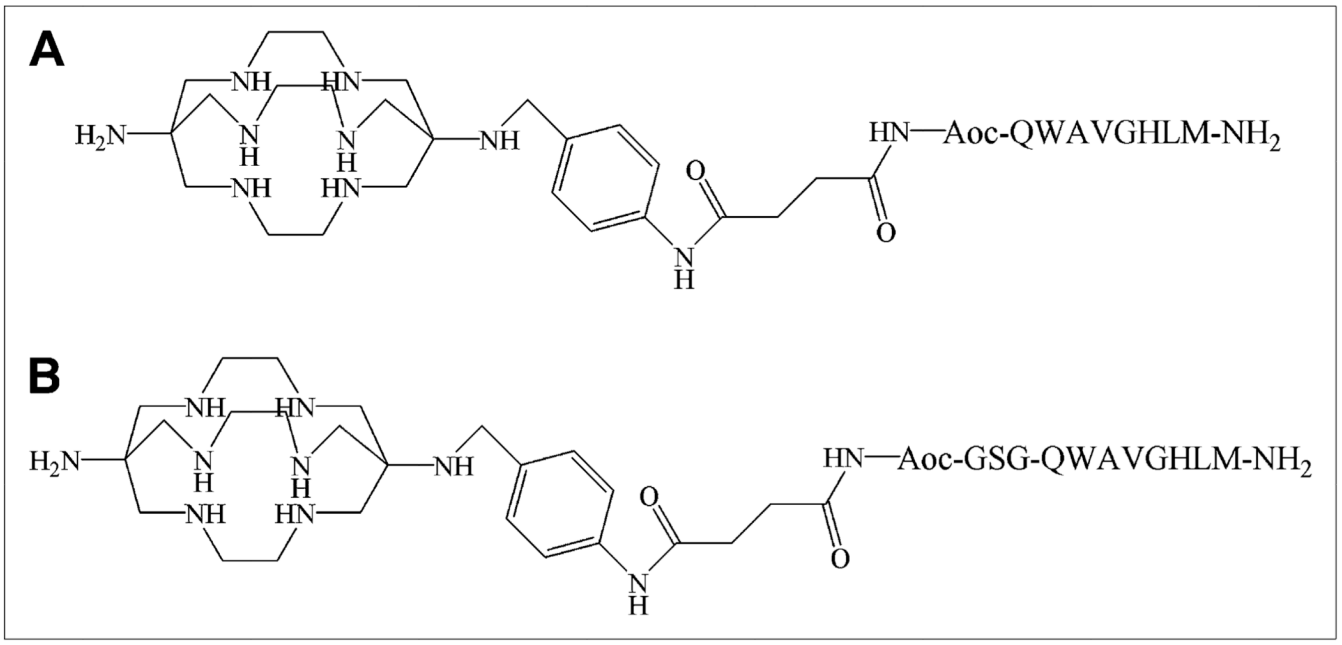

FIGURE 1.
Structures and amino acid sequences of ^{64}Cu-SarAr-SA-Aoc-bombesin(7–14) (A) and ^{64}Cu-SarAr-SA-Aoc-GSG-bombesin(7–14) (B).

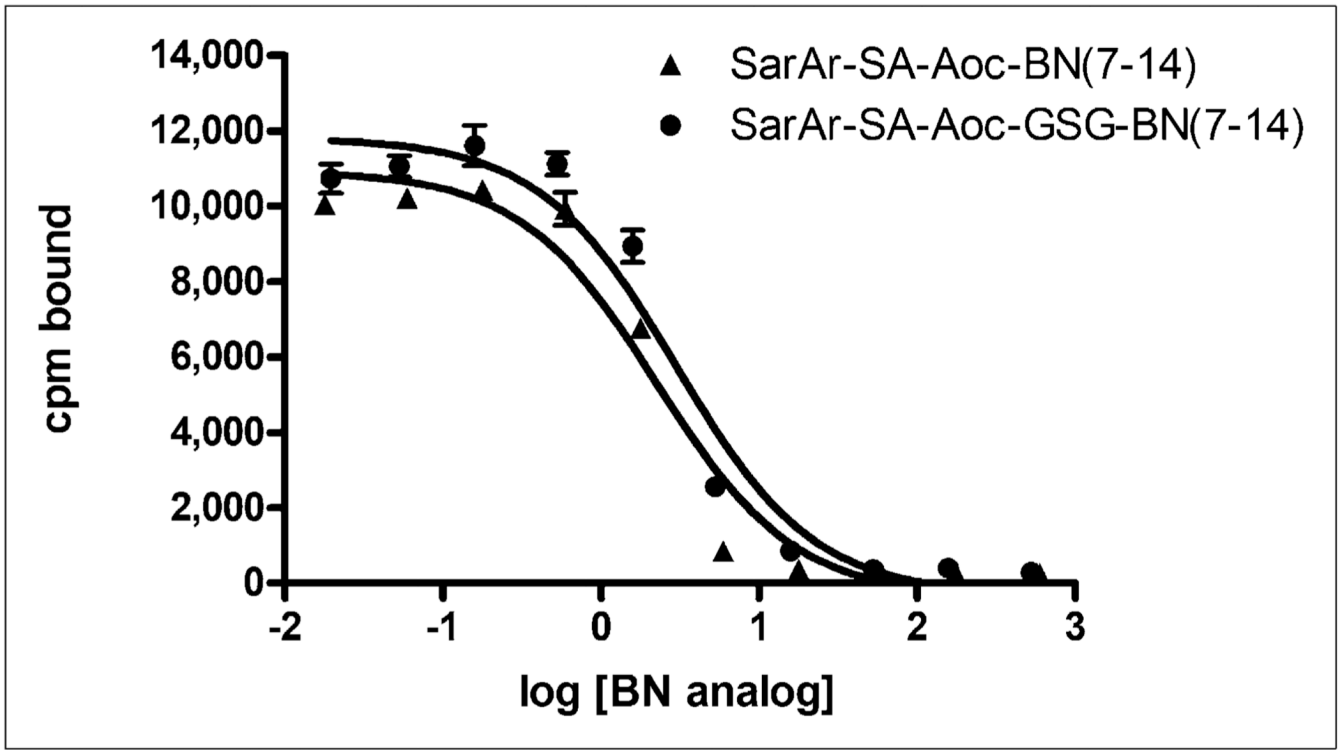

FIGURE 2.

Inhibition of ^{125}I-Tyr^{4}-bombesin binding to PC-3 cells with various concentrations of SarAr-SA-Aoc-bombesin(7–14) and SarAr-SA-Aoc-GSG-bombesin(7–14). Results of representative experiment are shown and expressed as counts per minute of radioactivity bound to cells vs. log of concentration (in nanomoles) of BN analogs. Data are presented as mean ± SEM of experiment, with each point being performed in triplicate. BN = bombesin; cpm = counts per minute.

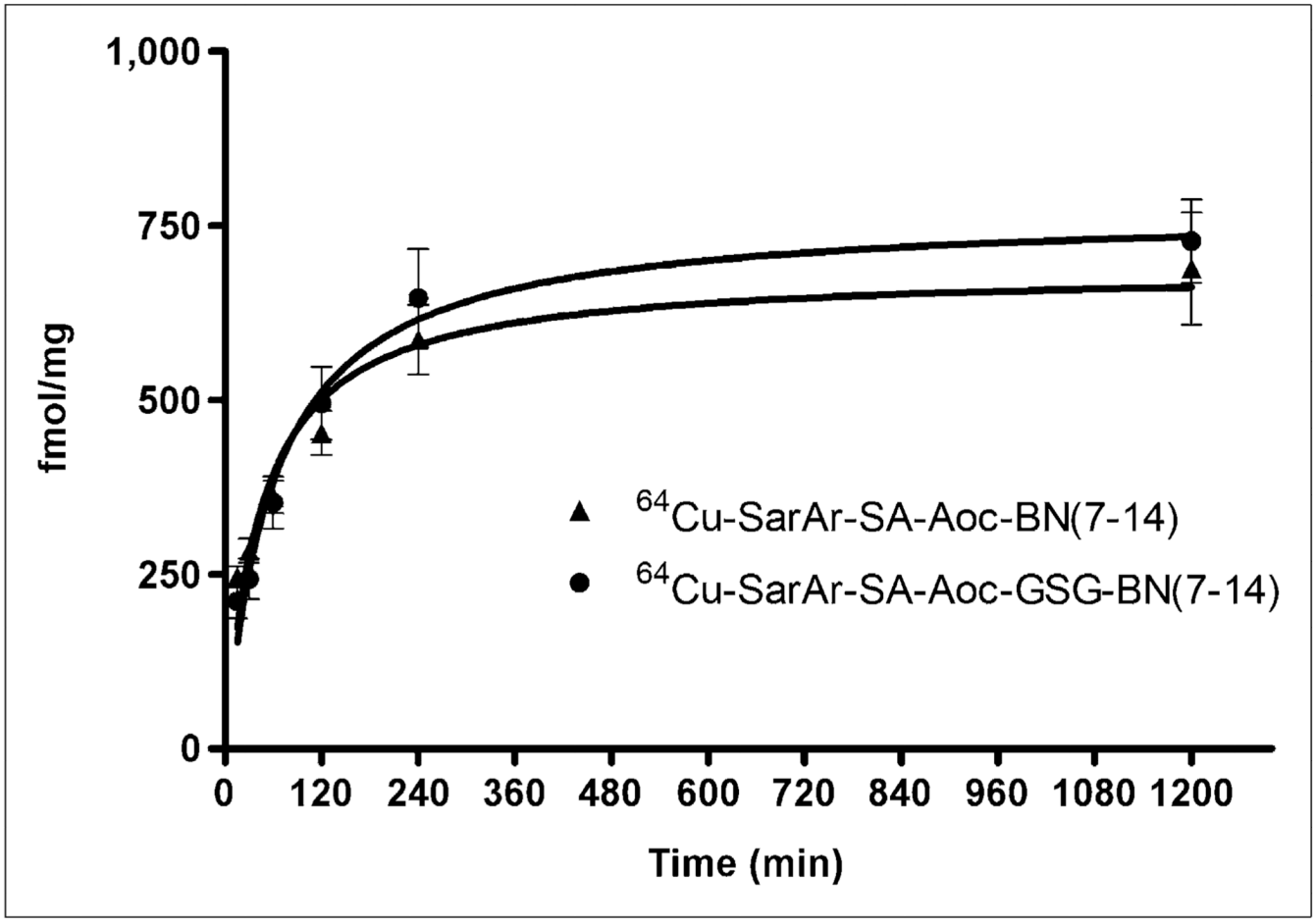

FIGURE 3.

Internalization of ^{64}Cu-SarAr-SA-Aoc-bombesin(7–14) and ^{64}Cu-SarAr-SA-Aoc-GSG-bombesin(7–14) into PC-3 cells. Cells were incubated with ^{64}Cu-labeled analogs for various times with or without Tyr^4-bombesin as inhibitor. After being acid-washed to remove cell-surface radioactivity, cells were lysed and collected, and amount of internalized radioactivity was counted. Data are shown as mean of 3 experiments ± SEM, with each experiment being performed in triplicate. BN = bombesin.

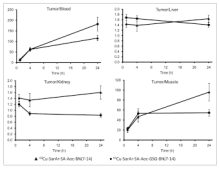

FIGURE 4.

Tumor-to-blood, tumor-to-liver, tumor-to-kidney, and tumor-to-muscle ratios for ^{64}Cu-SarAr-SA-Aoc-bombesin(7–14) and ^{64}Cu-SarAr-SA-Aoc-GSG-bombesin(7–14) in mice bearing PC-3 xenografts. Data are expressed as mean ± SEM of tumor-to-tissue ratio for each mouse (n = 5).

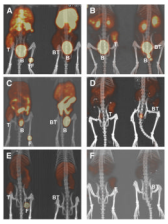

FIGURE 5.
Coronal views of maximum-intensity projections of small-animal PET images with coregistered CT image of mice bearing PC-3 xenografts in rear flank at 1 (A and B), 4 (C and D), and 24 h (E and F). Mice were injected intravenously with ^{64}Cu-SarAr-SA-Aoc-bombesin(7–14) (A, C, and E; tumors on left flank) and ^{64}Cu-SarAr-SA-Aoc-GSG-bombesin(7–14) (B, D, and F; tumors on right flank). Mice on left of each frame were not injected with blocking agent, whereas mice on right received 100 μg of Tyr^4-bombesin as inhibitor. Fiducial markers (F) are also shown in some images. B = bladder; BT = blocked tumors; T = nonblocked tumors.

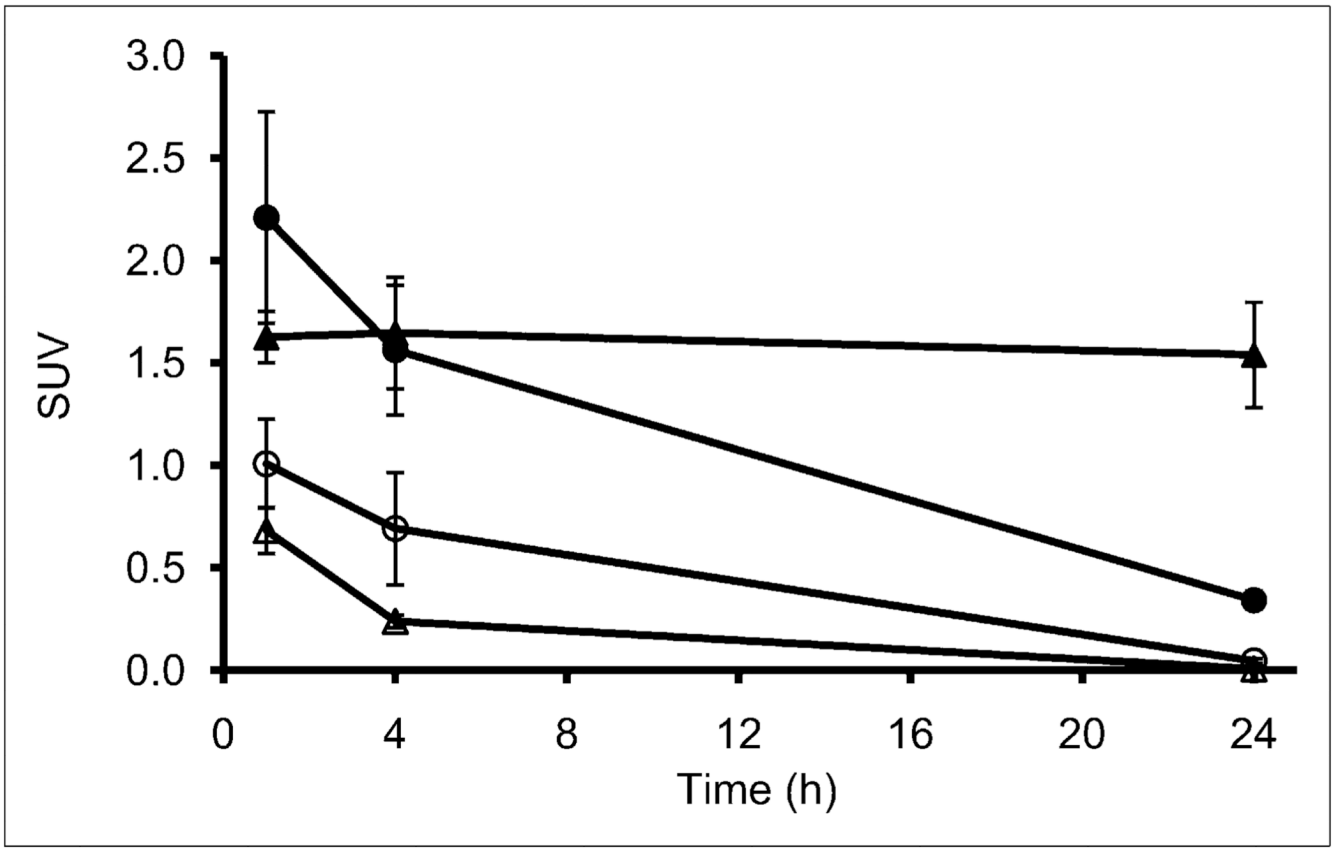

FIGURE 6.

Standardized uptake values for tumor uptake of ^{64}Cu-SarAr-SA-Aoc-bombesin(7–14) ▲ and △) and ^{64}Cu-SarAr-SA-Aoc-GSG-bombesin(7–14) (● and ○) over time as determined by small-animal PET. Open symbols represent ^{64}Cu-labeled analog that was coinjected with blocking agent. Imaging data represent mean ± SEM of 3 mice per group.

J Nucl Med. Author manuscript; available in PMC 2011 May 6.

TABLE 1

Biodistribution of ^{64}Cu-SarAr-SA-Aoc-Bombesin(7–14) and ^{64}Cu-SarAr-SA-Aoc-GSG-Bombesin(7–14) in Mice Bearing PC-3 Tumors (% ID/g ± SEM; n = 5) at 1, 4, and 24 Hours

	^{64}Cu-SarAr-SA-Aoc-bombesin(7–14)			^{64}Cu-SarAr-SA-Aoc-GSG-bombesin(7–14)		
Tissue	**1 h**	**4 h**	**24 h**	**1 h**	**4 h**	**24 h**
Blood	0.936 ± 0.165	0.181 ± 0.031	0.072 ± 0.009	0.769 ± 0.032	0.080 ± 0.007	0.024 ± 0.005
Lung	1.246 ± 0.106	0.679 ± 0.028	0.367 ± 0.026	1.241 ± 0.062	0.348 ± 0.017	0.216 ± 0.014
Liver	9.467 ± 1.435	8.263 ± 0.452	4.681 ± 0.289	5.061 ± 0.285	2.959 ± 0.138	2.824 ± 0.274
Spleen	1.233 ± 0.186	3.185 ± 1.210	0.970 ± 0.184	1.507 ± 0.063	1.073 ± 0.066	0.931 ± 0.091
Kidney	9.367 ± 0.898	8.303 ± 0.558	5.159 ± 0.284	7.076 ± 0.268	5.532 ± 0.459	4.731 ± 0.198
Muscle	0.923 ± 0.274	0.272 ± 0.077	0.095 ± 0.017	0.392 ± 0.022	0.093 ± 0.003	0.074 ± 0.008
Bone	1.740 ± 0.525	0.815 ± 0.035	0.469 ± 0.025	1.411 ± 0.335	0.533 ± 0.022	0.498 ± 0.040
Pancreas	67.392 ± 4.573	48.422 ± 5.250	36.935 ± 3.770	52.036 ± 4.423	29.540 ± 1.158	29.888 ± 1.599
Tumor	13.015 ± 0.932	10.805 ± 1.091	7.365 ± 0.911	8.541 ± 0.806	4.913 ± 0.571	3.937 ± 0.322